On Transverse Shear Stiffness of Composites Laminates

Wenbin Yu*
Purdue University, West Lafayette, IN 47907-2045, USA

I. Introduction

Composite laminates are commonly modeled using plate (for flat laminates) or shell (for curved laminates) elements (see Figure 1). Although there are many higher-order models including higher-order equivalent single-layer models, zig-zag models, and layerwise models developed in the literature[1] derived using the axiomatic method, variational asymptotic method, and formal asymptotic method, commercial FEA codes often provide two equivalent single-layer models: the Kirchhoff-Love model and the Reissner-Mindlin model. In this note, I will first provide a simple introduction to these two models according to [2], then I will focus on how to compute the corresponding plate stiffness for these two models with or without smearing properties, particularly the transverse shear stiffness for the Reissner–Mindlin model.

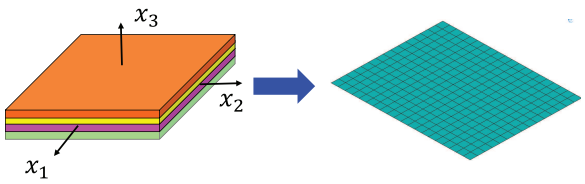

Figure 1. Model a composite laminate using a plate model.

II. Kirchhoff–Love Model

The Kirchhoff plate model, also referred to as the classical plate model, was originally developed by Kirchhoff for thin plates made of isotropic materials. It is based on a set of a priori assumptions, including that the transverse normal material line (described by the coordinate x_3) along the thickness direction is rigid, remains straight and perpendicular to the reference surface (described by coordinates x_1 and x_2) during deformation. Furthermore, the model assumes that the structure experiences a plane-stress state during deformation.

Love later extended these assumptions to curved panels, resulting in the classical shell model. Since both models share the same assumptions and constitutive relations, they are collectively referred to as the Kirchhoff-Love model. For simplicity, we focus on the plate model below.

The kinematics of the Kirchhoff–Love model involves three displacements ($\bar{u}_1, \bar{u}_2, \bar{u}_3$), as well as six strain variables including in-plane strains ($\epsilon_{11}, \epsilon_{22}, \epsilon_{12}$) and curvatures ($\kappa_{11}, \kappa_{22}, \kappa_{12}$). Specifically for a plate, the strain–displacement relations are

$$\begin{aligned} \epsilon_{11} &= \frac{\partial \bar{u}_1}{\partial x_1}, \qquad \epsilon_{22} = \frac{\partial \bar{u}_2}{\partial x_2}, \qquad 2\epsilon_{12} = \frac{\partial \bar{u}_1}{\partial x_2} + \frac{\partial \bar{u}_2}{\partial x_1} \\ \kappa_{11} &= -\frac{\partial^2 \bar{u}_3}{\partial x_1^2}, \qquad \kappa_{22} = -\frac{\partial^2 \bar{u}_3}{\partial x_2^2}, \qquad \kappa_{12} = -\frac{\partial^2 \bar{u}_3}{\partial x_1 \partial x_2} \end{aligned} \tag{1}$$

The kinetics of the Kirchhoff–Love model involves six stress resultants: in-plane force resultants (N_{11}, N_{22}, N_{12})

*Milton Clauser Professor, School of Aeronautics and Astronautics, ASME Fellow, ASC Fellow, and AIAA Associate Fellow.

and moment resultants (M_{11}, M_{22}, M_{12}). These are governed by the following equilibrium equations:

$$\begin{aligned}
&\frac{\partial N_{11}}{\partial x_1} + \frac{\partial N_{12}}{\partial x_2} + p_1 = 0 \\
&\frac{\partial N_{12}}{\partial x_1} + \frac{\partial N_{22}}{\partial x_2} + p_2 = 0 \\
&\frac{\partial^2 M_{11}}{\partial {x_1}^2} + \frac{\partial^2 M_{22}}{\partial {x_2}^2} + 2\frac{\partial^2 M_{12}}{\partial x_1 \partial x_2} + \frac{\partial q_2}{\partial x_1} - \frac{\partial q_1}{\partial x_2} + p_3 = 0
\end{aligned} \tag{2}$$

Here, p_1, p_2, and p_3 represent equivalent forces per unit area in the three directions, and q_1 and q_2 are equivalent moments per unit area in the two in-plane directions, distributed over the reference surface.

The constitutive relations for the Kirchhoff–Love model are expressed as:

$$\begin{Bmatrix} N_{11} \\ N_{22} \\ N_{12} \\ M_{11} \\ M_{22} \\ M_{12} \end{Bmatrix} = \begin{bmatrix} A_{11} & A_{12} & A_{16} & B_{11} & B_{12} & B_{16} \\ A_{12} & A_{22} & A_{26} & B_{21} & B_{22} & B_{26} \\ A_{16} & A_{26} & A_{66} & B_{61} & B_{62} & B_{66} \\ B_{11} & B_{21} & B_{61} & D_{11} & D_{12} & D_{16} \\ B_{12} & B_{22} & B_{62} & D_{12} & D_{22} & D_{26} \\ B_{16} & B_{26} & B_{66} & D_{16} & D_{26} & D_{66} \end{bmatrix} \begin{Bmatrix} \epsilon_{11} \\ \epsilon_{22} \\ 2\epsilon_{12} \\ \kappa_{11} \\ \kappa_{22} \\ 2\kappa_{12} \end{Bmatrix} \tag{3}$$

This 6×6 matrix is termed the stiffness matrix for the Kirchhoff–Love model, and its inverse is the compliance matrix. The submatrices A, B, and D are well-known in the classical laminate theory (CLT)[a] with A as the in-plane stiffness, D as the bending stiffness, and B as the coupling stiffness between in-plane and bending behavior. Although B is symmetric in CLT, it is not necessarily symmetric for general anisotropic heterogeneous panels. For special composite panels, such as symmetric laminates, B vanishes, decoupling the bending behavior from the in-plane behavior.

Eqs. (1), (2), and (3) form a system of 15 equations underpinning the Kirchhoff–Love model to be solved along with boundary conditions for 15 unknowns: three displacements, six strain variables, and six stress resultants. Kinematics and kinetics remain the same for homogeneous or heterogeneous plates made of isotropic or anisotropic materials. The only difference is that the stiffness matrix in Eq. (3) could be fully populated for anisotropic homogeneous or heterogeneous panels.

Although the Kirchhoff–Love model was originally developed based on a priori assumptions, these assumptions are not strictly necessary. Advanced modeling techniques, such as the mechanics of structure genome (MSG) [2], can derive this model with using these a priori assumptions. Thus, in this note, the Kirchhoff–Love model refers to the system of 15 field variables governed by the 15 equations in Eqs. (1), (2), and (3), regardless of the derivation method. This system of equations are implemented in most commercial FEA codes.

III. Reissner–Mindlin Model

When the thickness of the panel is not sufficiently small compared to its in-plane dimensions, or when the deformation cannot be adequately captured using only the in-plane strains and curvatures, a more refined model is needed. The Reissner–Mindlin model, named after the independent contributions of Reissner and Mindlin, addresses these limitations and extends the capabilities of the Kirchhoff–Love model.

The kinematics of the Reissner–Mindlin model includes three displacement variables ($\bar{u}_1, \bar{u}_2, \bar{u}_3$), two rotation variables (θ_1, θ_2), and eight strain variables including the in-plane strains ($\epsilon_{11}, \epsilon_{22}, \epsilon_{12}$), the curvatures ($\kappa_{11}, \kappa_{22}, \kappa_{12}$), and the transverse shear strains ($\epsilon_{13}, \epsilon_{23}$). For a plate, the strain–displacement relations are given by

$$\begin{aligned}
&\epsilon_{11} = \frac{\partial \bar{u}_1}{\partial x_1}, \qquad \epsilon_{22} = \frac{\partial \bar{u}_2}{\partial x_2}, \qquad 2\epsilon_{12} = \frac{\partial \bar{u}_1}{\partial x_2} + \frac{\partial \bar{u}_2}{\partial x_1} \\
&\kappa_{11} = \frac{\partial \theta_2}{\partial x_1}, \qquad \kappa_{22} = -\frac{\partial \theta_1}{\partial x_2}, \qquad 2\kappa_{12} = \frac{\partial \theta_2}{\partial x_2} - \frac{\partial \theta_1}{\partial x_1} \\
&2\epsilon_{13} = \frac{\partial \bar{u}_3}{\partial x_1} + \theta_2, \qquad 2\epsilon_{23} = \frac{\partial \bar{u}_3}{\partial x_2} - \theta_1
\end{aligned} \tag{4}$$

[a]Kirchhoff–Love model is not the same as CLT. Only when one uses the Kirchhoff-Love kinematic assumptions along with the plane-stress assumption to derive a Kirchhoff-Love model for composite laminates, it becomes CLT.

The kinetics of the Reissner–Mindlin model involves eight stress resultants including in-plane force resultants (N_{11}, N_{22}, N_{12}), moment resultants (M_{11}, M_{22}, M_{12}), and transverse shear force resultants (N_{13}, N_{23}). These stress resultants are governed by the following five equilibrium equations:

$$\begin{aligned}
&\frac{\partial N_{11}}{\partial x_1} + \frac{\partial N_{12}}{\partial x_2} + p_1 = 0 \\
&\frac{\partial N_{12}}{\partial x_1} + \frac{\partial N_{22}}{\partial x_2} + p_2 = 0 \\
&\frac{\partial N_{13}}{\partial x_1} + \frac{\partial N_{23}}{\partial x_2} + p_3 = 0 \\
&\frac{\partial M_{12}}{\partial x_1} + \frac{\partial M_{22}}{\partial x_2} - q_1 - N_{23} = 0 \\
&\frac{\partial M_{11}}{\partial x_1} + \frac{\partial M_{12}}{\partial x_2} + q_2 - N_{13} = 0
\end{aligned} \tag{5}$$

The constitutive relations for the Reissner–Mindlin model are expressed as:

$$\begin{Bmatrix} N_{11} \\ N_{22} \\ N_{12} \\ M_{11} \\ M_{22} \\ M_{12} \\ N_{13} \\ N_{23} \end{Bmatrix} = \begin{bmatrix} A_{11} & A_{12} & A_{16} & B_{11} & B_{12} & B_{16} & Y_{11} & Y_{12} \\ A_{12} & A_{22} & A_{26} & B_{21} & B_{22} & B_{26} & Y_{21} & Y_{22} \\ A_{16} & A_{26} & A_{66} & B_{61} & B_{62} & B_{66} & Y_{31} & Y_{32} \\ B_{11} & B_{21} & B_{61} & D_{11} & D_{12} & D_{16} & Y_{41} & Y_{42} \\ B_{12} & B_{22} & B_{62} & D_{12} & D_{22} & D_{26} & Y_{51} & Y_{52} \\ B_{16} & B_{26} & B_{66} & D_{16} & D_{26} & D_{66} & Y_{61} & Y_{62} \\ Y_{11} & Y_{21} & Y_{31} & Y_{41} & Y_{51} & Y_{61} & G_{11} & G_{12} \\ Y_{12} & Y_{22} & Y_{32} & Y_{42} & Y_{52} & Y_{62} & G_{12} & G_{22} \end{bmatrix} \begin{Bmatrix} \epsilon_{11} \\ \epsilon_{22} \\ 2\epsilon_{12} \\ \kappa_{11} \\ \kappa_{22} \\ 2\kappa_{12} \\ 2\epsilon_{13} \\ 2\epsilon_{23} \end{Bmatrix} \tag{6}$$

This 8×8 matrix is called the stiffness matrix, and its inverse is the compliance matrix for the Reissner–Mindlin model. G_{ij} $(i = 1, 2; j = 1, 2)$ denotes the transverse shear stiffness, and Y_{ij} $(i = 1, \ldots, 6; j = 1, 2)$ denotes the coupling stiffness among the in-plane strains and curvatures and transverse shear strains. The matrices A, B, and D may differ from those in Eq. (3) due to possible nonzero Y_{ij} terms. None of existing commercial FEA codes currently handle nonzero Y_{ij} terms. Thus, these terms are often not computed and neglected.

Eqs. (4), (5), and (6) form a system of 21 equations underpinning the Reissner–Mindlin model to be solved with appropriate boundary conditions for 21 unknowns: five displacement variables, eight strain variables, and eight stress resultants. Kinematics and kinetics remain unchanged regardless whether the panel is homogeneous or heterogeneous, made of isotropic or anisotropic materials. The only difference lies in the stiffness matrix in Eq. (6), which can be fully populated for anisotropic homogeneous or heterogeneous panels.

Although the Reissner–Mindlin model was originally developed using a priori assumptions, these assumptions are not strictly necessary. Advanced modeling techniques, such as MSG, can also derive this model without these a priori assumptions. Thus, the Reissner–Mindlin model described here refers to the system of 21 field variables governed by the 21 equations in Eqs. (4), (5), and (6), independent of the derivation method.

IV. Plate Stiffness for Composite Laminates without Smearing Properties

For composite laminates (see Figure 2 for a sketch and thickness coordinates setup), regardless of which method of derivation is used[1], it is well-established that

$$A = \langle\langle Q \rangle\rangle, \qquad B = \langle\langle x_3 Q \rangle\rangle, \qquad D = \left\langle\left\langle x_3^2 Q \right\rangle\right\rangle \tag{7}$$

where Q is the plane-stress reduced stiffness matrix relating in-plane stresses and strains, and the double angle brackets indicate integration through the thickness, that is $\langle\langle \cdot \rangle\rangle = \int_{\frac{-h}{2}}^{\frac{h}{2}} \cdot \mathrm{d}x_3$. For laminates, we are dealing with piecewise functions through the thickness due to different layers. The integration can be explicitly

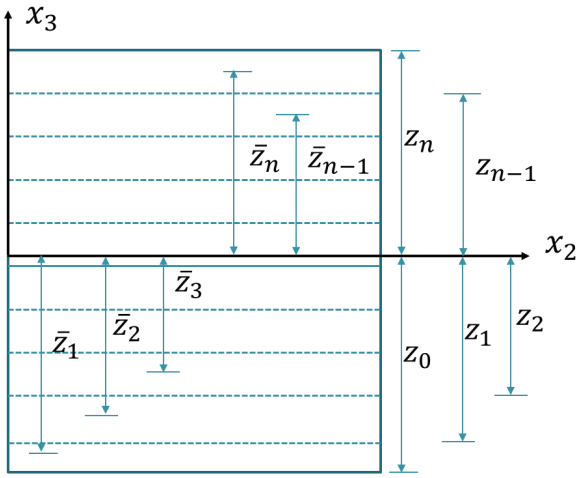

Figure 2. Laminate thickness coordinates.

written as

$$\langle\langle f \rangle\rangle = \sum_{i=1}^{n} \int_{z_{i-1}}^{z_i} f^{(i)} \mathrm{d}x_3 \tag{8}$$

where f is a generic function, and $f^{(i)}$ is f defined over $x_3 \in [z_{i-1}, z_i]$, h is the total thickness of the laminate and the origin of the thickness coordinate is located at the center here for simplicity, not necessity. If the thickness coordinate is not originated at the center, these stiffness matrices can be easily modified as shown in [2].

A simple way of computing the shear stiffness matrix is provided by the first-order shear deformation theory (FOSDT)[b]. For monoclinic materials with the $x_1 - x_2$ plane as the plane of symmetry and material coordinates rotating about x_3, transverse normal stress couples to in-plane stresses only. The reduced stiffness matrix due to plane-stress assumption can be expressed using Q and C_s with

$$\sigma_s = C_s \varepsilon_s \tag{9}$$

where

$$\sigma_s = \begin{Bmatrix} \sigma_{13} \\ \sigma_{23} \end{Bmatrix}, \qquad C_s = \begin{bmatrix} C_{55} & C_{45} \\ C_{45} & C_{44} \end{bmatrix}, \qquad \varepsilon_s = \begin{Bmatrix} 2\varepsilon_{13} \\ 2\varepsilon_{23} \end{Bmatrix}$$

where C_{44}, C_{45}, C_{55} are terms in the corresponding 6×6 3D stiffness matrix. Substituting Eq. (9) into the definition of plate transverse shear stress resultants in FOSDT, we obtain

$$N_s = G_s \gamma \tag{10}$$

where

$$N_s = \begin{Bmatrix} N_{13} \\ N_{23} \end{Bmatrix}, \qquad G_s = K \begin{bmatrix} \langle\langle C_{55} \rangle\rangle & \langle\langle C_{45} \rangle\rangle \\ \langle\langle C_{45} \rangle\rangle & \langle\langle C_{44} \rangle\rangle \end{bmatrix}, \qquad \gamma = \begin{Bmatrix} 2\epsilon_{13} \\ 2\epsilon_{23} \end{Bmatrix} \tag{11}$$

Eq. (6) simplifies to be:

$$\begin{Bmatrix} N \\ M \\ N_s \end{Bmatrix} = \begin{bmatrix} A & B & 0 \\ B^T & D & 0 \\ 0 & 0 & G_s \end{bmatrix} \begin{Bmatrix} \epsilon \\ \kappa \\ \gamma \end{Bmatrix} \tag{12}$$

Comparing Eq. (12) to Eq. (6), we observe that there are no couplings between transverse shear and other deformation modes (i.e., $Y_{ij} = 0$). This is primarily due to the restriction of laminates made of monoclinic

[b]Reissner–Mindlin model is not the same as FOSDT. Only when one uses the assumptions associated with CLT and constant shear strain assumption and introduces the shear correction factor to derive a Reissner–Mindlin model, it becomes FOSDT.

layers without couplings between the transverse shear deformation modes and other deformation modes. Here, G_s denotes the *transverse shear stiffness*. A correction factor K, commonly called the *shear correction factor*, is introduced to correct for the over-prediction of strain energy due to the assumption of constant transverse shear strains through the thickness. Due to constant transverse shear strain assumption, the transverse shear stresses will be layerwise constant which will make the structure artificially stiffer than the real structure. The shear correction factor should be computed so that the strain energy due to the assumed constant shear stresses is the same as the real transverse stresses. For isotropic homogeneous plates, $K = 5/6$. For composite laminates, we usually do not know the value of K although 5/6 is commonly suggested for convenience[3]. Sometimes, K is used as a free parameter to improve the predictions of FOSDT when it is compared to more accurate predictions obtained using 3D FEA, higher-order models, or experiments. There are other ways to compute the shear correction factors proposed in the literature[4–7].

MSG provides a unique way of computing the transverse shear stiffness without introducing the shear correction factors. The resulting Reissner-Mindlin model is as accurate as the fourth-order zig-zag model (assuming that the displacements are fourth-order polynomials for each layer) without introducing the assumptions associated with FOSDT[8].The corresponding shear stiffness can be computed analytically although a bit tedious if there are many layers. The MSG-based Reissner–Mindlin model has been implemented in SwiftComp to compute the plate stiffness in terms of A, B, D, and G_s and recover 3D stresses based on the plate behavior predicted from commercial FEA codes[2].

V. Plate Stiffness for Composite Laminates with Smearing Properties

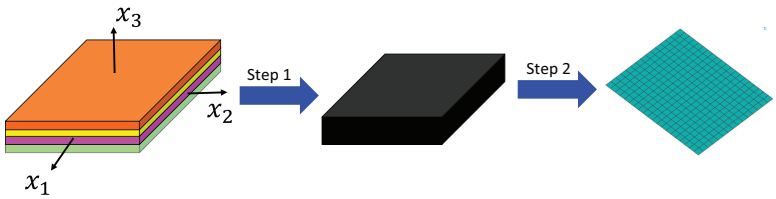

Figure 3. Homogenization of a laminate as an equivalent homogeneous solid, and then as a plate.

During initial sizing of composite laminates for realistic aerospace structures, the specific stacking sequence is not available. All we know is the percentage of layers of different angles. Without providing a specific stacking sequence for the laminate, the best we can do is to homogenize it to be a 3D anisotropic, homogeneous body as shown in the Step 1 of Figure 3. As it is proven by MSG[2,9], the exact solution for this step corresponds to assuming both the in-plane strains and out-of-plane stresses constant throughout all the layers. This approach allows treating a composite laminate as if it were made of black-colored aluminum and still using conventional structural design tools to carry out a geometry design with material selections. **This approach is only valid for symmetric laminates subjected to in-plane loads. For nonsymmetric laminates or laminates under bending loads, this approach should be avoided. However, if the laminate is a sub-laminate which is repeating many times (say more than ten) inside the entire laminate, it is still reasonable according to the mechanics of structure genome[2] to use this approach to compute the effective 3D properties of the sub-laminate and assume the entire laminate is made of the same imaginary homogeneous material, even if the laminate is not symmetric or not solely subjected to in-plane loads**. The double-double laminates advocating by Dr. Steve Tsai in recent years is essentially making laminates to better satisfy the latter condition, which can be termed as the homogeneity condition for composite laminates.

Assuming that each layer is homogeneous and generally anisotropic, the constitutive relations of each layer can be written as

$$\begin{Bmatrix} \varepsilon_e \\ \varepsilon_t \end{Bmatrix} = \begin{bmatrix} S_e & S_{et} \\ S_{et}^T & S_t \end{bmatrix} \begin{Bmatrix} \sigma_e \\ \sigma_t \end{Bmatrix} \tag{13}$$

with $\sigma_e = \lfloor \sigma_{11} \;\; \sigma_{22} \;\; \sigma_{12} \rfloor^T$, $\sigma_t = \lfloor \sigma_{33} \;\; \sigma_{23} \;\; \sigma_{13} \rfloor^T$, $\varepsilon_e = \lfloor \varepsilon_{11} \;\; \varepsilon_{22} \;\; 2\varepsilon_{12} \rfloor^T$, $\varepsilon_t = \lfloor \varepsilon_{33} \;\; 2\varepsilon_{23} \;\; 2\varepsilon_{13} \rfloor^T$, and

$$S_e = \begin{bmatrix} S_{11} & S_{12} & S_{16} \\ S_{12} & S_{22} & S_{26} \\ S_{16} & S_{26} & S_{66} \end{bmatrix}, \qquad S_{et} = \begin{bmatrix} S_{13} & S_{14} & S_{15} \\ S_{23} & S_{24} & S_{25} \\ S_{36} & S_{46} & S_{56} \end{bmatrix}, \qquad S_t = \begin{bmatrix} S_{33} & S_{34} & S_{35} \\ S_{34} & S_{44} & S_{45} \\ S_{35} & S_{45} & S_{55} \end{bmatrix}$$

The smeared properties can be computed as

$$Q^* = \langle Q \rangle, \qquad S^*_{et} = Q^{*-1} \langle Q S_{et} \rangle, \qquad S^*_t = \left\langle S_t - S^T_{et} Q S_{et} \right\rangle + S^{*T}_{et} Q^* S^*_{et} \tag{14}$$

with $Q = S_e^{-1}$, corresponding to the plane-stress reduced stiffness matrix in CLT and the single angle brackets indicate the average over the thickness. For composite laminates, f is a piecewise constant for each layer. The average is computed as

$$\langle f \rangle = \frac{1}{h} \sum_{i=1}^{n} t_i f_i$$

where t_i is the thickness for each layer, f_i is the property for each layer, and n is the total number of layers. Clearly, the origin of the thickness coordinate and the layers can be located anywhere without affecting the calculation of smeared properties.

Finally, the effective compliance matrix can be rearranged into the order according to the engineering notation so that

$$\begin{Bmatrix} \bar{\varepsilon}_{11} \\ \bar{\varepsilon}_{22} \\ \bar{\varepsilon}_{33} \\ 2\bar{\varepsilon}_{23} \\ 2\bar{\varepsilon}_{13} \\ 2\bar{\varepsilon}_{12} \end{Bmatrix} = \begin{bmatrix} S^*_{11} & S^*_{12} & S^*_{13} & S^*_{14} & S^*_{15} & S^*_{16} \\ & S^*_{22} & S^*_{23} & S^*_{24} & S^*_{25} & S^*_{26} \\ & & S^*_{33} & S^*_{34} & S^*_{35} & S^*_{36} \\ & & & S^*_{44} & S^*_{45} & S^*_{46} \\ & \text{symmetric} & & & S^*_{55} & S^*_{56} \\ & & & & & S^*_{66} \end{bmatrix} \begin{Bmatrix} \bar{\sigma}_{11} \\ \bar{\sigma}_{22} \\ \bar{\sigma}_{33} \\ \bar{\sigma}_{23} \\ \bar{\sigma}_{13} \\ \bar{\sigma}_{12} \end{Bmatrix} \tag{15}$$

from which, one can obtain the effective stiffness matrix:

$$\begin{Bmatrix} \bar{\sigma}_{11} \\ \bar{\sigma}_{22} \\ \bar{\sigma}_{33} \\ \bar{\sigma}_{23} \\ \bar{\sigma}_{13} \\ \bar{\sigma}_{12} \end{Bmatrix} = \begin{bmatrix} C^*_{11} & C^*_{12} & C^*_{13} & C^*_{14} & C^*_{15} & C^*_{16} \\ & C^*_{22} & C^*_{23} & C^*_{24} & C^*_{25} & C^*_{26} \\ & & C^*_{33} & C^*_{34} & C^*_{35} & C^*_{36} \\ & & & C^*_{44} & C^*_{45} & C^*_{46} \\ & \text{symmetric} & & & C^*_{55} & C^*_{56} \\ & & & & & C^*_{66} \end{bmatrix} \begin{Bmatrix} \bar{\varepsilon}_{11} \\ \bar{\varepsilon}_{22} \\ \bar{\varepsilon}_{33} \\ 2\bar{\varepsilon}_{23} \\ 2\bar{\varepsilon}_{13} \\ 2\bar{\varepsilon}_{12} \end{Bmatrix} \tag{16}$$

Although one can model the 3D anisotropic homogeneous body using 3D solid elements in the structural analysis during sizing, plate elements is often used to further reduce the computational cost. In other words, we need to compute the corresponding plate stiffness based on the effective 3D properties (see Step 2 of Figure 3). Now, the plate can be considered as containing just one effective layer with Q^*, and we can compute

$$A = Q^* h, \qquad B = 0, \qquad D = \frac{h^2}{12} A$$

with A the same as what is computed in CLT.

If the composite lamina is monoclinic in the laminate coordinate system with $S_{14} = S_{15} = S_{24} = S_{25} = S_{34} = S_{35} = S_{46} = S_{56} = 0$, we can also show $S^*_{14} = S^*_{15} = S^*_{24} = S^*_{25} = S^*_{34} = S^*_{35} = S^*_{46} = S^*_{56} = 0$ and $C^*_{14} = C^*_{15} = C^*_{24} = C^*_{25} = C^*_{34} = C^*_{35} = C^*_{46} = C^*_{56} = 0$.

According to FOSDT, we can compute the transverse shear stiffness as

$$G_s = K \begin{bmatrix} C^*_{55} & C^*_{45} \\ C^*_{45} & C^*_{44} \end{bmatrix} h$$

with $K = 5/6$ as suggested by [3].

VI. Conclusion Remarks

Stiffness of composite laminates (A, B, D and G) can be accurately calculated if the stacking sequence is known. The computation of A, B, D are well established and the results are the same as CLT. There are difference approaches to compute G with or without introducing shear correction factors. Accurate computation of G requires capturing the layerwise varying shear strains and stresses within the laminate.

If the stacking sequence is not available, as is the case of the current sizing practice, smearing property approach should be used. However, as pointed out previously and it is worth repeating. Smearing property approach only works under the following two situations:

1. The laminate is symmetric and subject to in-plane loads.

2. The stack is a sub-laminate and the entire laminate contains many repetitions of this sub-laminate.

For Situation 1, D and G will not enter the calculation and thus do not matter.

On the contrary, if you still need bending behavior, the smeared D and G will be misleading because it could introduce significant errors. For example, a four-layer laminate with lamina constants $E_1 = 20 \times 10^6$ psi, $E_2 = 1.45 \times 10^6$ psi, $G_{12} = 10^6$ psi, $\nu_{12} = 0.3$, and $\nu_{23} = 0.49$ and layer thickness $t = 0.005$" will have $D_{11} = 11.86 \times 10^6$ lb·in and 2.53×10^6 lb·in for a laminate with a stacking sequence 0/90/90/0 and 90/0/0/90, respectively.

For the situations other than the aforementioned two, I would like to suggest two following ideas:

1. If there are only a few stacking sequences allowed by manufacturing, computing in-plane properties (corresponding to A), flexural properties (corresponding to D), and shear properties (corresponding to G) for different stacking sequences. During sizing, we can treat different stacking sequences as different material types for selection.

2. If there are many possible stacking sequences, what was suggested in item 1 is not cost effective. Instead, it might make more sense to have a statistic description of D and G. If we run through all possible stacking sequences (these calculations are very efficient), we can get a statistic distribution of D and G with a mean and standard deviation and other statistic descriptors if necessary, which can be further propagated into the structural analysis to obtain a statistic description of the results. Even if we do not carry out a full-blown uncertainty quantification, we can at least bound the structural responses by identifying the lower bound and upper bounds of D and G.

References

[1]Yu, W., "A Review of Modeling Methods of Composite Structures," *Materials*, Vol. 17, No. 2, 2024, 116007.

[2]Yu, W., *Multiscale Structural Mechanics: Top-Down Modeling of Composite Structures using Mechanics of Structure Genome*, Wiley, 1st ed., 2026.

[3]Reddy, J. N., *Mechanics of Laminated Composite Plates and Shells: Theory and Analysis*, CRC Press, Boca Raton, Florida, 2004.

[4]Whitney, J. M., "Shear Correction Factors for Orthotropic Laminates Under Static Load," *Journal of Applied Mechanics*, Vol. 40, 1973, pp. 302–304.

[5]Cohen, G. A., "Transverse Shear Stiffness of Laminated Anisotropic Shells," *Computer Methods in Applied Mechanics and Engineering*, Vol. 13, 1977, pp. 205–220.

[6]Goyal, V. K. and Kapania, R. K., "Ashear-deformable beam element for the analysis of laminated composites," *Finite Elements in Analysis and Design*, Vol. 43, 2007, pp. 463–477.

[7]Bednarcyk, B. A., Aboudi, J., Yarrington, P. W., and Collier, C. S., "Simplified Shear Solution for Determination of the Shear Stress Distribution in a Composite Panel from the Applied Shear Resultant," *Proceedings of the 49th Structures, Structural Dynamics and Materials Conference, Schaumburg, Illionois*, AIAA, Reston, Virginia, April 7 – 10, 2008, AIAA Paper 2008-2168.

[8]Demasi, L. and Yu, W., "Assess the Accuracy of the Variational Asymptotic Plate and Shell Analysis (VAPAS) Using the Generalized Unified Formulation (GUF)," *Mechanics of Advanced Materials and Structures*, Vol. 20, 2013, pp. 227–241.

[9]Yu, W., "An Exact Solution for Micromechanical Analysis of Periodically Layered Composites," *Mechanics Research Communications*, Vol. 46, 2012, pp. 71–75.